THE JOURNAL OF PHYSICAL CHEMISTRY B

Article

pubs.acs.org/JPCB

A Comparative Study of the Rotational Dynamics of PF_6^- Anions in the Crystals and Liquid States of 1-Butyl-3-methylimidazolium Hexafluorophosphate: Results from ^{31}P NMR Spectroscopy

Takatsugu Endo,[†] Hiroki Murata,[‡] Mamoru Imanari,[§] Noriko Mizushima,[∥] Hiroko Seki,[§] Sabyasachi Sen,[†] and Keiko Nishikawa*[,‡]

[†]Department of Chemical Engineering and Materials Science, The University of California, Davis, One Shield Avenue, Davis, California 95616, United States

[‡]Graduate School of Advanced Integration Science, Chiba University, 1-33 Yayoi-cho, Inage-ku, Chiba 263-8522, Japan

[§]Chemical Analysis Center, Chiba University, 1-33 Yayoi-cho, Inage-ku, Chiba 263-8522, Japan

[∥]Laboratory of Clinical Pharmacy, Yokohama College of Pharmacy, Matano-cho 601, Totsuka, Yokohama 245-0066, Japan

ABSTRACT: The rotational dynamics of the hexafluorophosphate anion (PF_6^-) in the crystalline and liquid states of the archetypal room temperature ionic liquid (RTIL) 1-butyl-3-methylimidazolium hexafluorophosphate ($[C_4mim]PF_6$) are investigated using ^{31}P NMR spectroscopy line shape analyses and spin−lattice relaxation time measurements. The PF_6^- anion performs isotropic rotation in all three polymorphic crystals phases α, β, and γ as well as in the liquid state with a characteristic time scale that ranges from a few ps to a few hundred ps over a temperature range of 180−280 K. The rotational correlation time τ_c for PF_6^- rotation follows the sequence γ-phase < α-phase ≈ liquid < β-phase. On the other hand, in the liquid state, all local motions in the cation as well as its global rotational reorientation are characterized by time scales that are slower compared to that for the PF_6^- anion rotation. The time scale τ_c and the activation energy of PF_6^- rotation in this RTIL are found to be comparable with those observed in ordinary alkali and ammonium salts despite the large counterion size and low melting point of the former. The high sphericity of the PF_6^- ion is hypothesized to play an important role in the decoupling of its rotational dynamics that appear to be practically independent of the averaged cation−anion interaction.

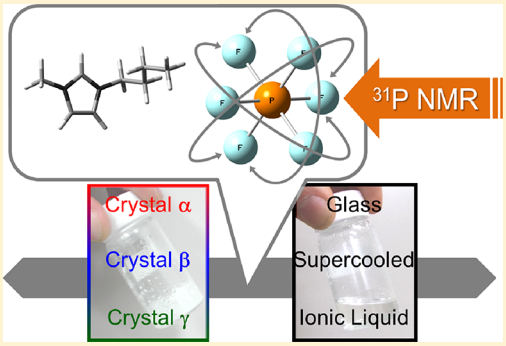

1. INTRODUCTION

Hexafluorophosphate (PF_6^-) is a representative anion in a wide variety of crystalline salts and ionic liquids. The dynamical behavior of the constituent ions is central in controlling the physical state and properties of these materials. Therefore, a fundamental mechanistic understanding of the PF_6^- rotational dynamics in the solid state for alkali salts,[1−5] ammonium salts,[6−14] and the other complex salts[15−26] has been the subject of intense investigation in the literature. As might be expected, the PF_6^- rotational dynamics depend on temperature as well as on the chemistry, structure, and phase state of the material in question. The anion rotates isotropically, rotates anisotropically, or shows freezing behavior depending on these variables.

In recent years, a new class of salts that has a melting point around or below room temperature, the so-called room temperature ionic liquids (RTILs), have been widely recognized and investigated.[27,28] Despite being salts, RTILs are liquids that have many attractive characters such as extremely low vapor pressure, negligible flammability, high thermal/chemical/electrochemical stability, unique solubility, and so forth. They are considered to be potentially useful as electrolytes and green solvents. There are numerous possible combinations of cations and anions, and RTILs typically containing organic cations are thereby easy to design, enabling fine control on their physicochemical properties. For this reason, RTILs are frequently regarded as "designer solvents".

PF_6^- is a typical anion in RTILs that, because of its relatively large size, often leads to the melting point of the salt at around or below room temperature. However, to the best of our knowledge, experimental studies on the PF_6^- rotational dynamics in RTILs are practically nonexistent in the liquid or the solid state except in a recent preliminary report by us.[29] Investigation of the PF_6^- dynamics in RTILs is important to understand not only the nature of a specific RTIL but also how RTILs are unique (or not) compared to ordinary salts. Additionally, since some RTILs containing PF_6^- anion crystallize near room temperature, it is possible to compare its rotational dynamics between the liquid and solid states, which is quite difficult for ordinary salts due to their tendency for decomposition before melting.

In the present work, one of the most representative RTILs, 1-butyl-3-methylimidazolium hexafluorophosphate ($[C_4mim]$-

Received: November 5, 2012
Revised: December 7, 2012
Published: December 14, 2012

PF_6, Figure 1), was selected. Its melting point is ca. 284 K, and it crystallizes around 243 K, exhibiting the cold crystallization.[30]

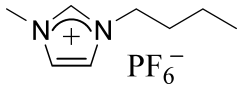

Figure 1. Chemical structure of $[C_4mim]PF_6$.

Recent studies have shown that this RTIL possesses complex thermal phase behavior and has three polymorphic crystals with the different butyl group conformations, namely, gauche−trans, trans−trans, and gauche′-trans.[30,31] The role of the PF_6^- dynamics may be critical in understanding this unique phase behavior. In this study, we use ^{31}P nuclear magnetic resonance (NMR) spectroscopic measurements to elucidate the nature of these dynamical processes in $[C_4mim]PF_6$ in its crystalline and liquid states.

2. EXPERIMENTAL SECTION

$[C_4mim]PF_6$ was purchased from Kanto Chemical Co., Inc. The sample was washed several times with distilled water, and the absence of halide ions was confirmed by the $AgNO_3$ test. The sample was dried at ca. 333 K for 1 day under 10^{-3} Pa before use and sealed in a 4 mm NMR tube in a vacuum; this procedure reduces the water content of RTILs to less than 150 ppm.[32]

NMR measurements were performed using a spectrometer (ECX400, JEOL) operating at a ^{31}P resonance frequency of 162 MHz. The temperature of the sample was calibrated using methanol and glycerin.[33−36] Heating or cooling rates of 5−10 K/min were used to change the sample temperature. The ^{31}P NMR spin−lattice relaxation time T_1 was measured over a range of temperatures with the inversion recovery method except for the crystalline β phase. This phase is relatively unstable against its eventual transformation to the γ phase and has a long T_1. Thus, the saturation recovery method was used for the measurement of the ^{31}P T_1 for this phase in order to shorten the measurement time. The experimental ^{31}P second moment M_2 values at different temperatures were estimated from the free induction decay (FID) signals measured with the Hahn echo method (90−τ−180) using the following equations[37]

$$M(t) = M_0 \exp\left(-\frac{a^2}{2}t^2\right)\frac{\sin bt}{bt} \quad (1)$$

$$M_2 = \frac{1}{\gamma_I^2}\left(a^2 + \frac{1}{3}b^2\right) \quad (2)$$

where $M(t)$ and M_0 are the sample magnetization at times t and t = 0, respectively, and γ_I is the gyromagnetic ratio of the ^{31}P nucleus. This method mainly refocuses the dipole−dipole coupling of heteronuclear spins. A nonlinear regression method (Levenberg−Marquardt) was used for theoretical fitting of the FID and T_1 data.

Density functional theory (DFT) calculations of the optimization of the crystal structures were performed using the Gaussian 09 program package.[38] Full geometry optimization analyses for ions in the gas phase were carried out using 6-311+G(d,p) basis sets on the basis of Becke's three-parameter hybrid method[39] with the LYP correlation (B3LYP)[40,41] for lighter atoms than Kr. For the heavier atoms, SDD basis sets were used. The calculations in the gas phase are known to provide useful insights into the structure and dynamics of RTILs.[42−45] No imaginary frequencies were produced by the optimized structures; this ensured the presence of an energetic minimum. Ionic volumes of the cations in a wide range of salts containing anion were estimated using DFT calculations.[46] Since ionic volume calculations in the Gaussian 09 program are based on the Monte Carlo method, such calculations were repeated 15 times for the monatomic ions and 5 times for polyatomic ions and the average values are reported.

3. RESULTS AND DISCUSSION

3.1. Thermal Phase Behavior. In a recent study using simultaneous measurement of Raman spectroscopy/calorimetry[47] and NMR spectroscopy, it has been demonstrated that $[C_4mim]PF_6$ has the three crystalline polymorphs, namely, the α, β, and γ phases.[30,31] The α phase was the first crystalline phase obtained from the supercooled liquid state. Although the crystallization did not occur during cooling from room temperature to ca. 177 K, it occurred during subsequent heating from 177 K (i.e., cold crystallization) around 233 K. The α phase changes to the β phase around 253 K on further heating. Finally, the γ phase was obtained from the β phase after the latter was kept for several hours at any temperature between 220 and 280 K. These solid−solid phase transitions are all found to be irreversible.

3.2. ^{31}P Second Moment M_2. The temperature dependence of the second moment M_2 of NMR line shapes that are controlled by dipolar coupling carries important information regarding the dynamical characteristics of the nuclide that result in motional line narrowing. In general, M_2 is the variance and is represented as

$$M_2 = \frac{\int(\omega - M_1)^2 f(\omega)\, d\omega}{\int f(\omega)\, d\omega} \quad (3)$$

where M_1 is the first moment. The theoretical rigid lattice ^{31}P M_2 values are calculated for $[C_4mim]PF_6$ in the crystalline state using the Van Vleck equation[48]

$$M_2 = \frac{3}{5}\gamma_I^2\hbar^2N^{-1}I(I+1)\sum_{j,k} r_{jk}^{-6} + \frac{4}{15}\gamma_S^2\hbar^2N^{-1} S(S+1)\sum_{j,f} r_{jf}^{-6} \quad (4)$$

where $\hbar$ is the reduced Planck's constant, N is the number of nuclei, I and S are the nuclear spin quantum numbers for ^{31}P and heteronuclear spins, respectively, r is the distance between spin pairs j and k or j and f, and γ_I and γ_S are the gyromagnetic ratios of ^{31}P and heteronuclear spins, respectively. These calculations are carried out only for the γ phase with the gauche′−trans conformation of the cation[49] due to the lack of crystal structure data for the α and β phases. However, the ^{31}P M_2 values are expected to be similar for all three crystalline polymorphs, since the main contribution to M_2 for ^{31}P would come from the six ^{19}F nuclei that are directly bonded to the former in the PF_6^- anionic octahedron that have the same geometry irrespective of the crystal structure. The contributions to M_2 from the $^{31}P-^1H$ dipolar interactions are small but not negligible and may depend on the crystal structure of the specific polymorph. However, based on the findings in other RTILs that show crystal polymorphism,[50,51] the differences in the contributions from $^{31}P-^1H$ dipolar interaction between

dx.doi.org/10.1021/jp310947c | J. Phys. Chem. B 2013, 117, 326−332

Table 1. Theoretical Second Moment M_2 (Gauss^2) of ^{31}P in $[C_4mim]PF_6$ in the Crystalline State

			inter ^{31}P−^{19}F		inter ^{31}P−^{1}H		inter ^{31}P−^{31}P		
		intra ^{31}P−^{19}F	<6 Å	6 Å<	<6 Å	6 Å<	<6 Å	6 Å<	total
rigid lattice		51.45	0.10	0.05	1.40	0.15	0.005	0.004	53.16
3-CH_3 and δ-CH_3 free rotations		51.45	0.10	0.05	1.13	0.15	0.005	0.004	52.90
PF_6^- rotation	C_4	25.73	0.08	0.05	1.13	0.15	0.005	0.004	27.16
PF_6^- rotation	C_2	6.43	0.07	0.05	1.13	0.15	0.005	0.004	7.85
PF_6^- rotation	C_3	0.00	0.07	0.05	1.13	0.15	0.005	0.004	1.42
PF_6^- rotation	isotropic	0.00	0.07	0.05	1.13	0.15	0.005	0.004	1.42

different crystalline polymorphs should be on the order of 10% or less.[31] It should be noted here that the C−H distances in the cations in the crystal structure were obtained from DFT, since these C−H distances obtained from X-ray diffraction are generally underestimated.

The ^{31}P M_2 values are calculated as the sum of two contributions: one from distances ≤6.0 Å and the other from longer distances. The first contribution was calculated on the basis of the crystal structure.[49] The second contribution from larger distances was estimated using the following equation[52] in combination with eq 4 where the distance sums were approximated as

$$\sum_{j,k} r_{jk}^{-6}, \sum_{j,f} r_{jf}^{-6} = 4\pi N_p (3R^3V)^{-1} \quad (5)$$

This equation assumes a continuous distribution of nuclei at distances larger than the cutoff radius of 6.0 Å from the central ^{31}P nuclide. In eq 5, N_p is the number of nuclei per unit cell, R is the cutoff radius (6.0 Å), and V is the unit cell volume. Under rapid rotation of a pair of atoms whose relative positions remain unchanged during rotation, the M_2 value is reduced by a factor ρ that is given by[53,53]

$$\rho = \frac{1}{4}(3\cos^2\theta - 1)^2 \quad (6)$$

where θ is the angle between the internuclear vector and the rotation axis. The modification of the rigid lattice value of the ^{31}P M_2 by the six possible rotational motions in the $[C_4mim]PF_6$ crystal[31] are estimated. These rotational motions are the free rotation of the two methyl groups in the cation, three axial rotations of the PF_6^- anion with C_2, C_3, and C_4 symmetries, and the isotropic rotation of the anion. The ^{31}P M_2 value for the rigid lattice structure is found to be 53.16 G^2. This value reduces only slightly to 52.90 G^2 for rapid rotation of the two methyl groups. The axial rotations of the PF_6^- anion with C_4 and C_2 symmetries reduce M_2 significantly to 27.16 and 7.85 G^2, respectively. On the other hand, for rapid isotropic rotation of the anion or C_3 axial rotation, M_2 is drastically reduced to 1.42 G^2 with no contributions from the intra-anionic ^{31}P−^{19}F dipolar interactions. The ^{31}P M_2 values obtained from these calculations including the relative contributions of different heteronuclear dipolar couplings under various rotational motions are listed in Table 1.

Figure 2 shows the temperature dependence of the experimental ^{31}P M_2 values in all crystalline polymorphs obtained from the spin echo measurements. All ^{31}P M_2 values are below 1.42 G^2, suggesting that the contribution to M_2 from the intra-anionic ^{31}P−^{19}F dipolar interactions is negligible and only small interionic contributions remain. The negligible contribution from intra-anionic ^{31}P−^{19}F dipolar interactions implies that the PF_6^- anion undergoes rapid isotropic rotation

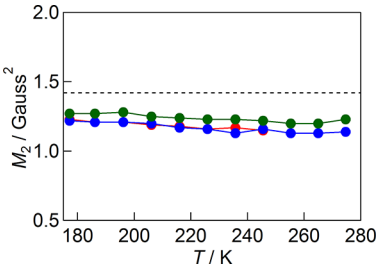

Figure 2. Temperature dependence of the second moment M_2 of ^{31}P NMR spectra. Red, blue, and green symbols represent data for the $[C_4mim]PF_6$ crystalline polymorphs α, β, and γ, respectively. The gray dashed line is the theoretical limit of M_2 of 1.42 G^2 for isotropic rotation of PF_6^- anions (see Table 1).

in all crystalline polymorphs. As noted above, rapid axial rotation of the anion with C_3 symmetry could also lead to such effects but would be unlikely, since there are no plausible strong interactions in the crystal that would allow for preferential rotation about the C_3 axis. The fact that all the experimental ^{31}P M_2 values are below 1.42 G^2 and they decrease slightly with increasing temperature is consistent with the hypothesis that there are rotational motions in the cation that exist in all three crystalline states which decrease the ^{31}P−^{1}H dipolar interactions. It is probable that the differences in the ^{31}P M_2 values originate from the differences in the crystal structures of the three polymorphs that change the ^{31}P−^{1}H dipolar interactions.

3.3. ^{31}P NMR Spin−Lattice Relaxation Time T_1. Figure 3 shows the temperature dependence of the ^{31}P T_1 for the three

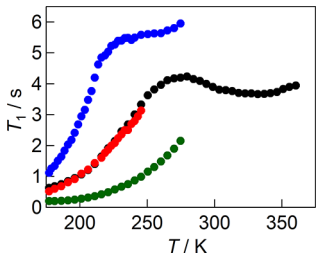

Figure 3. Temperature dependence of ^{31}P T_1 plots. Red, blue, green, and black symbols represent crystal polymorphs α, β, and γ and the liquid state of $[C_4mim]PF_6$, respectively.

crystalline polymorphs and the liquid of $[C_4mim]PF_6$. The data in all cases seem to have a minimum that is located below 170 K. In addition, a rather shallow minimum in ^{31}P T_1 is observed for the β phase and the liquid that is located near 250 and 330 K, respectively. A modeling of the T_1 data requires the consideration of all possible spin−lattice relaxation mechanisms for ^{31}P nuclides in this material. In general, there are five NMR interactions that may contribute to T_1 relaxation:

dx.doi.org/10.1021/jp310947c | J. Phys. Chem. B 2013, 117, 326−332

$$\frac{1}{T_1} = \frac{1}{T_1^{DD}} + \frac{1}{T_1^{CSA}} + \frac{1}{T_1^{SR}} + \frac{1}{T_1^{Sc}} + \frac{1}{T_1^{Q}} \quad (7)$$

where T_1^{DD}, T_1^{CSA}, T_1^{SR}, T_1^{Sc}, and T_1^{Q} are the relaxation times associated with magnetic dipole−dipole, chemical shift anisotropy, spin rotation, scalar, and quadrupole interactions, respectively. ^{31}P is a spin-1/2 nuclide that is located in the center of the PF_6^- anion with octahedral site symmetry and is characterized by negligible chemical shift anisotropy. Hence, the contribution to T_1 from chemical shift anisotropy, scalar, and quadrupole interactions can be safely neglected. Since T_1^{SR} must decrease with increasing temprature while the experimental ^{31}P T_1 shows an opposite trend for most of the low temperature range in Figure 3, the dominant interaction responsible for the spin−lattice relaxation of the ^{31}P nuclides in $[C_4mim]PF_6$ in this temperature range is clearly the intra-anionic ^{31}P−^{19}F heteronuclear dipolar coupling contribution to T_1^{DD}. As mentioned above, this dipolar coupling is averaged due to the rapid isotropic rotation of the PF_6^- anions in $[C_4mim]PF_6$ and this dynamical process must also be responsible for the spin−lattice relaxation of the ^{31}P nuclides in the low temperature region in Figure 3. On the basis of Table 1, interionic ^{31}P−^{1}H interactions are small but do exist in $[C_4mim]PF_6$, though the interionic ^{31}P−^{19}F and ^{31}P−^{31}P interactions can be negligile. Therefore, the minimum at high temperature in the ^{31}P T_1 observed for the β phase and for the liquid state (Figure 3) is assumed to originate from the interionic ^{31}P−^{1}H dipolar interaction as the cationic motion becomes appreciable with increasing temperature. It should be noted that the ^{31}P T_1 of the α and γ phases does not show a second minmum at high temperature, in contrast to the β phase and the liquid state. On the basis of our previous work,[31] their minmum is expected to appear at higher temperature (which is out of the available temperature range) than that of the β phase because of the slower cation rotational dynamics. Then, eq 7 can be rewritten as $1/T_1 = 1/T_1^{DD(P-F)} + 1/T_1^{DD(P-H)}$, where T_1^{DD} for heteronuclear dipolar coupling can be written as[37,54]

$$\frac{1}{T_1^{DD}} = C[J(\omega_I - \omega_S) + 3J(\omega_I) + 6J(\omega_I + \omega_S)] \quad (8)$$

$$C = \frac{1}{2}\gamma_I^2 \Delta M_2 \quad (9)$$

$$J(\omega) = \frac{2\tau_c}{1 + (\omega\tau_c)^2} \quad (10)$$

$$\tau_c = \tau_0 \exp\left(\frac{E_a}{RT}\right) \quad (11)$$

In these equations, $J(\omega)$ is the spectral density, ΔM_2 is a part of the second moment averaged by the considered motion, τ_c is the rotational correlation time of the PF_6^- anion for $T_1^{DD(P-F)}$ and that of the vectors joining ^{31}P and ^{1}H nuclides in the anion and the surrounding cations for $T_1^{DD(P-H)}$, τ_0 is the correlation time at infinite temperature, E_a is the activation energy for the rotational dynamics, ω_I and ω_S are the resonance frequencies for ^{31}P and ^{19}F or ^{1}H, respectively, and R is the universal gas constant. The ^{31}P T_1 data were fitted using these equations, where τ_0, E_a, and ΔM_2 were used as fitting parameters except the ΔM_2 value in $1/T_1^{DD(P-F)}$ is fixed to be 51.5 G^2 corresponding to the rigid lattice intra-anionic ^{31}P−^{19}F dipolar interaction (*vide supra*). This is because using ΔM_2 as a fitting parameter is difficult due to the lack of any observable T_1 minimum for $1/T_1^{DD(P-F)}$ in the low temperature region (Figure 3). The resulting fits are shown in Figure 4, and the corresponding fitting parameters τ_0, E_a, and ΔM_2 are summrized in Table 2. The temperature dependence of the τ_c values for all samples are shown in Figure 5. For example, the values of α, β, and γ phases and the liquid state are estimated to be 31.1 ± 3.0, 10.5 ± 5.9, 153.0 ± 27.2, and 31.3 ± 7.0 ps, respectively, at 200 K. Although, to the best of our knowledge, this is the first report of τ_c and E_a for PF_6^- rotation in the crystal polymorphs of $[C_4mim]PF_6$, for the liquid, our results are in good agreement with those reported in previous experimental and computational studies.[29,57,58]

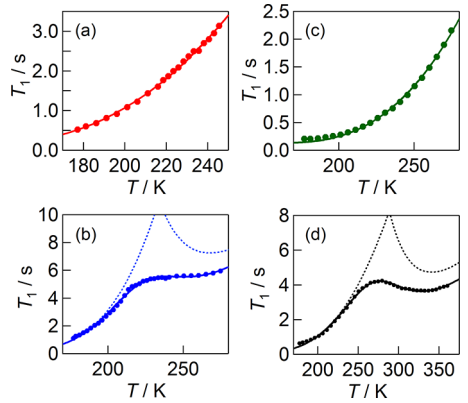

Figure 4. Fits (solid lines) of eqs 8−11 to the measured ^{31}P T_1 data (symbols) in Figure 3 for $[C_4mim]PF_6$: (a) α-phase; (b) β-phase; (c) γ-phase; (d) the liquid. The individual simulation components in parts b and d are indicated by dashed lines.

The ΔM_2 values of 1.0 and 1.6 G^2 are obtained from the simulation of the high temperature T_1 minimum (Figure 4) for the β phase and the liquid, respectively. These ΔM_2 values are comparable with the contributions to the ^{31}P M_2 from interionic ^{31}P−^{1}H dipolar coupling (see Table 1), suggesting that the high temperature component of ^{31}P T_1 in Figure 3 is associated with segemental motion of the cation that modulates the ^{31}P−^{1}H dipolar interactions. It should be noted that the assignments of the dynamical processes of the constituent ions to ^{31}P T_1 in $[C_4mim]PF_6$ in this work are different from those reported in our previous work.[29] In our previous work on the $[C_4mim]PF_6$ liquid, it was assumed that the motional process associated with the ^{31}P T_1 below 170 K was PF_6^- librational motion and that associated with the high temperature T_1 minimum was the PF_6^- isotropic rotation. These assignments were tentative, as ^{31}P T_1 data for the liquid were not available above 290 K. In light of the new data presented in this study over a wide range of temperatures, it seems appropriate to explain that the T_1 component observed at lower temperature orignates from isotropic rotation of the anion and that at higher temperature comes from rotational motions of the functional groups of the cation.

3.4. Comparative Analysis of the PF_6^- Dynamics in Crystalline and Liquid States. The results presented above, when taken together, clearly demonstrate that RTILs are unique materials that enable comparison of ionic dynamics in salts between crystalline and liquid states. As can be seen in Figure 5, the time scale τ_c for the rotational dynamics of the PF_6^- anion in all phases is on the order of picoseconds and is the slowest in the γ phase and the fastest in the β phase. The α phase and the liquid are comparable in their behavior and are

dx.doi.org/10.1021/jp310947c | J. Phys. Chem. B 2013, 117, 326−332

Table 2. Parameters τ_0, E_a, and ΔM_2 in eqs 8−11 (See Text) Derived from Fitting the T_1 Data (See Figure 4)

	crystal α	crystal β		crystal γ	liquid	
interaction	P−F	P−F	P−H	P−F	P−F	P−H
ΔM_2 (Gauss^2)	51.5 (fixed)	51.5 (fixed)	1.0 ± 0.0	51.5 (fixed)	51.5 (fixed)	1.6 ± 0.0
E_a (kJ mol^{-1})	9.7 ± 0.1	14.4 ± 0.6	17.2 ± 1.6	13.9 ± 0.2	11.1 ± 0.3	20.2 ± 0.9
τ_0 (fs)	92 ± 6	2 ± 1	311 ± 241	35 ± 4	38 ± 6	572 ± 186
motional assignment	PF_6^- isotropic rotation	PF_6^- isotropic rotation	rotational motion in the cation	PF_6^- isotropic rotation	PF_6^- isotropic rotation	rotational motion in the cation

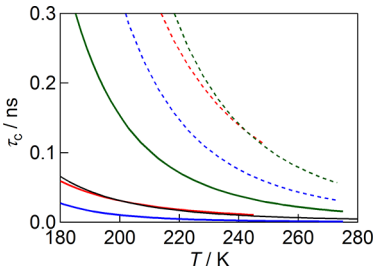

Figure 5. Rotational correlation times τ_c in $[C_4mim]PF_6$ derived from fits to the ^{31}P T_1 data. Solid and dashed lines are for rotation of PF_6^- and δ-CH_3, respectively. Red, crystal α; blue, crystal β; green, crystal γ; black, the liquid state. The data for δ-CH_3 are taken from a previous report in the literature.[31]

characterized by time scales intermediate between those characteristic of the β and γ phases (Figure 5). It was shown in a previous study[29] that the τ_c of PF_6^- rotation in the supercooled $[C_4mim]PF_6$ liquid increases only slightly with decreasing temperature to several tens of picoseconds even below its glass transition (192 K), indicating that this dynamics is not related to the viscous slowdown and is strongly decoupled from the structural relaxation process. The slowest τ_c of PF_6^- rotation in the γ phase is consistent with the fact that this phase has the strongest cation−anion interaction and the slowest rotational motions of the cation[31] among all three crystal polymorphs (*vide infra*). These dynamical properties may be responsible for the highest stability of the γ phase among the three crystalline states. The cation−anion Coulombic interaction should be weaker in the liquid state compared to that in the solid state due to the increase in molar volume by ∼10−15%[57,58] that typically accompanies melting. Therefore, one may expect faster ionic dynamics in the liquid state. However, the present results show that τ_c of PF_6^- rotation in the liquid state is comparable to that in the α phase and is slower than the β phase (Figure 5). Such behavior may be related to the fact that the PF_6^- rotational dynamics is governed by the local structure and/or local interactions rather than the average Columbic interaction between the cations and the anions.

It is worth comparing the anion dynamics to that of the cation in the $[C_4mim]PF_6$ crystals. Figure 5 compares the τ_c of the δ-CH_3 rotational motion in the cation with the τ_c of PF_6^- rotation in the crystalline polymorphs of $[C_4mim]PF_6$.[31] Interestingly, the trend of the τ_c for the rotational motion is the same for both cation and anions. The PF_6^- rotational motion in the three crystal phases is all faster than the δ-CH_3 rotation in cations. Our previous results indicated that δ-CH_3 rotation was slower than the rotation of the methyl group attached to the imidazolium ring (3-CH_3) but faster than the segmental motion of the butyl group.[31,59] Hence, the order of τ_c for the rotational motion in the $[C_4mim]PF_6$ crystals is 3-CH_3 < PF_6^- < δ-CH_3 < butyl group segmental motion. The presence of multiple time scales may suggest the presence of a dynamical hierarchy in these materials. A similar comparison between the cation and anion rotational dynamics can also be made in the case of the $[C_4mim]PF_6$ liquid for which previous studies investigated the cation dynamics.[60−63] The τ_c of PF_6^- rotation in the liquid state as obtained in this study is 3.3 ps at

Table 3. E_a and τ_0 (If Available) for Rotational Motion of PF_6^- Anions in Various Salts in the Crystalline State as Reported in the Literature and the Ionic Volumes of the Corresponding Cations Calculated Using DFT in This Study[a]

salts	E_a (kJ mol^{-1})/τ_0 (s) of PF_6^-	cation volume (Å^3)
$LiPF_6$	20/-[4]	0.4
$NaPF_6$	23.0/-,[2] 31.0/8.3 × 10^{-16},[4] 16.7/6.1 × 10^{-14},[4] 33.1/3 × 10^{-16},[5] 28.9/2 × 10^{-15} [5]	1.1
KPF_6	8.4/-,[1] 24.3/5.4 × 10^{-15},[3] 26.8/1.8 × 10^{-15},[3] 28.0/8.9 × 10^{-17},[3] 46.0/5 × 10^{-21},[5] 21.3/9 × 10^{-15} [5]	3.8
$RbPF_6$	6.7/1.4 × 10^{-11},[3] 8.8/7.2 × 10^{-13},[3] 16.7/1.1 × 10^{-15},[3] 17.6/2 × 10^{-16},[5] 6.3/9 × 10^{-12} [5]	6.3
$CsPF_6$	3.2/1.4 × 10^{-10},[4] 6.7/1.0 × 10^{-13},[4] 10.5/1.2 × 10^{-16},[4] 3.1/5.3 × 10^{-13} [4]	15.9
NH_4PF_6	14.6/-[9]	9.6
ND_4PF_6	23.0/1.5 × 10^{-18},[7] 17.2/5.9 × 10^{-16},[7] 17.2/3.7 × 10^{-16},[8] 18.4/5.2 × 10^{-17} [8]	8.5
NH_4PF_6 NH_4F	24.3/3.3 × 10^{-15},[6] 12.6/5.8 × 10^{-13} [6]	49.0
$[(CH_3)_4N]PF_6$	15/6 × 10^{-15},[12] 15/6 × 10^{-15} [14]	91.2
$[(CH_3)_3NC_2H_5]PF_6$	5/-,[13] 12/-[13]	107.2
$[C(NH_2)_3]PF_6$	26/2 × 10^{-13},[19] 23.5/3.50 × 10^{-14},[22] 27.4/1.13 × 10^{-14} [22]	58.5
$[Sb(CH_3)_4]PF_6$	10.4/2.36 × 10^{-12},[23] 5.8/2.09 × 10^{-15} [23]	112.1
$[C_4H_8NH_2]PF_6$	10/-[26]	80.9
$[C_5H_{10}NH_2]PF_6$	15/-[25]	91.2
$[C_5H_5NH]PF_6$	9/4.5 × 10^{-13} [24]	77.0
$[Cu(paphy)Cl](PF_6)$ H_2O[b]	5.8/-[20]	203.8
$[C_4mim]PF_6$ (this work)	9.7/92 × 10^{-15}, 14.4/2 × 10^{-15}, 13.9/35 × 10^{-15}	148.8

[a]The ionic volume of PF_6^- was estimated to be 71.3 Å^3 in all cases. [b]paphy = pyridine-2-carboxaldehyde-2-pyridylhydrazone.

dx.doi.org/10.1021/jp310947c | J. Phys. Chem. B 2013, 117, 326−332

300 K, whereas, for the cation at the same temperature in the liquid state, τ_c was found in previous studies to range between 700 and 900 ps for the three carbons in the imidazolium ring, 26 ps for 3-CH_3, 510/220/120 or 168/103/60 ps for the three carbons in the methylene group of the butyl chain, and 26 or 13 ps for the rotation of δ-CH_3.[60,62,63] Therefore, it is clear that all local motions in the cation have a slower rotational time scale compared to that for PF_6^-. This conclusion is also true when the anion dynamics is compared to the rotational reorientation of the whole cation, as the latter is expectedly significantly slower with τ_c of ~3−4 ns near 300 K.[29,57,58,64−66] Previous NMR spectroscopy[67] and MD simulation[55,56] studies indicated that in contrast with the rotational dynamics the time scales of the translational dynamics of the cation and the anion were comparable.

Finally, it is interesting to compare the time scale of the PF_6^- rotational dynamics in $[C_4mim]PF_6$ to that in "ordinary" salts such as alkali and ammonium salt, as significant data are available in the literature on the PF_6^- rotational dynamics in such ordinary salts. Table 3 and Figure 6 compare E_a, τ_0 (if

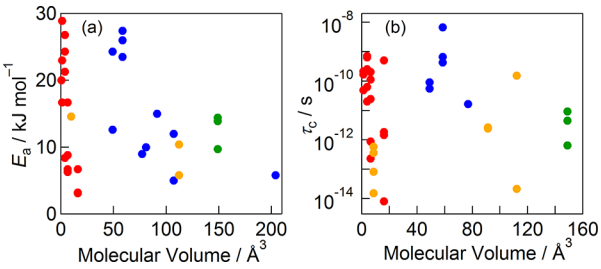

Figure 6. (a) E_a and (b) τ_c at 300 K for PF_6^- rotation in ordinary salts in their crystalline states. Red, yellow, blue, and green symbols represent data for salts with alkali cations, spherical nonalkali cations, nonspherical cations, and for $[C_4mim]PF_6$, respectively. The τ_c values for some salts were obtained by minor extrapolation, as their melting points are below 300 K. See Table 3 and references therein for further information. Note that part a does not include E_a values paired with unrealistically small τ_0 (below fs) in Table 3 because too small τ_0 tends to give high E_a.

available), and the ionic volume of the PF_6^- anion in these salts. The DFT calculations carried out in this study yield the ionic volumes of $[C_4mim]^+$ and PF_6^- ions to be 148.8 and 71.3 Å^3, respectively. These values are comparable to the van der Waals volumes of these ions that were reported in the literature to be 150 and 69 Å^3.[68] It is intuitively expected and was suggested in a number of previous studies that the ionic volume or radius is roughly correlated with PF_6^- rotational dynamics.[2,5,14,23] This is because larger ionic volume can decrease cation−anion interaction that could result in faster PF_6^- rotational dynamics. However, the data in Figure 6 indicate almost no relationship between the ionic volume and the dynamical parameters for the PF_6^- rotational dynamics. This observation strongly suggests that the PF_6^- rotational dynamics is not significantly influenced by the averaged cation−anion interaction. It is tempting to attribute this result to the high sphericity of the octahedral PF_6^- anions. Sphericity (Ψ), or the ratio of the surface area of a sphere with the same volume as the molecule to the actual surface area of the molecule, is given by[69]

$$\Psi = \pi^{1/3}(6V)^{2/3}/A \quad (12)$$

where V is the volume and A is the surface area and $\Psi = 1$ indicates a perfect sphere. For an octahedron, $\Psi \sim 0.85$, comparable to the sphericity of cage molecules such as As_4S_3 ($\Psi = 0.82$). It is well-known that ions or molecules with spherical symmetry are expected to have small activation barriers for rotational jumps or diffusion,[70−72] consistent with the activation energies of 10−15 kJ mol^{-1} obtained in this study (Table 2) for the isotropic rotation of PF_6^- anions in the $[C_4mim]PF_6$ crystals and liquid. Such low activation energies have also been observed for the rotational motion of these anions in a remarkably wide variety of salts, as shown in Figure 6 and listed in Table 3.

4. CONCLUSION

The PF_6^- anions display isotropic rotation in the crystalline polymorphs and in the liquid state of $[C_4mim]PF_6$. PF_6^- dynamics with a correlation time τ_c ranging between a few ps and a few hundred ps was studied over a temperature range of 180−280 K. The correlation times and their temperature dependences are found to be distinct for the three crystalline polymorphs, while the dynamics in the liquid is similar to that in the α-phase. The order of τ_c follows the sequence crystal γ > crystal $\alpha \approx$ liquid > crystal β such that the crystal γ has the slowest rotational motion. This result is consistent with the observation that crystal γ is the most stable polymorph among the three crystal phases. It is demonstrated that among the local and global motions in the constituent ions the rotational motion of PF_6^- in the $[C_4mim]PF_6$ liquid is the fastest except for the local 3-CH_3 rotation. The anion dynamics in $[C_4mim]PF_6$ are also compared to that in ordinary salts. Contrary to the intuitive expectation, the activation energy and τ_c for PF_6^- rotation in $[C_4mim]PF_6$ are comparable to those in ordinary salts with smaller counterion size and higher melting point. It is suggested that this behavior can be attributed to the high sphericity of the octahedral PF_6^- anions. We conclude that PF_6^- rotational motion is not significantly influenced by the averaged cation−anion interaction (i.e., Columbic interaction between a cation and the anion) but rather by more local interactions and crystal structure. The anion seems to not distinguish between RTILs and ordinary salts in terms of its rotational dynamics.

AUTHOR INFORMATION

Corresponding Author

*E-mail: k.nishikawa@faculty.chiba-u.jp.

Notes

The authors declare no competing financial interest.

ACKNOWLEDGMENTS

The present study was supported by the Ministry of Education, Culture, Sports, Science and Technology of Japan No. 21245003 Grant-in-Aid for Scientific Research (A) and the Global Center-of-Excellence Program "Advanced School for Organic Electronics". We also thank JSPS Postdoctoral Fellowships for Research Abroad.

REFERENCES

(1) Waugh, J. S. *Ann. N. Y. Acad. Sci.* **1958**, *70*, 900−926.
(2) Miller, G. R.; Gutowsky, H. S. *J. Chem. Phys.* **1963**, *39*, 1983−1994.
(3) Niemelä, L.; Niemelä, M.; Tuohi, J. *Ann. Acad. Sci. Fenn.* **1972**, *388*, 1.
(4) Niemelä, L.; Komu, M. *Ann. Acad. Sci. Fenn.* **1973**, *403*, 1.
(5) Gutowsky, H. S.; Albert, S. *J. Chem. Phys.* **1973**, *58*, 5446−5452.
(6) Todo, I.; Tatsuzaki, I. *Phys. Status Solidi* **1969**, *32*, 263−267.

(7) Niemela, L.; Tuohi, J. *Ann. Univ. Turku.* **1970**, *137*, A1.
(8) Albert, S.; Gutowsky, H. S. *J. Chem. Phys.* **1973**, *59*, 3585−3594.
(9) Svare, I.; el Hiah Abd el Haleem, A. *Phys. Scr.* **1979**, *19*, 351−354.
(10) Kaliaperumal, R.; Srinivasan, R.; Ramanathan, K. V. *Chem. Phys. Lett.* **1983**, *102*, 29−32.
(11) Kozlova, S. G.; Kriger, Y. G.; Samoilov, P. P.; Gabuda, S. P. *Phys. Status Solidi B* **1986**, *135*, K53−K56.
(12) Reynhardt, E. C.; Jurga, S.; Jurga, K. *Chem. Phys. Lett.* **1992**, *194*, 410−414.
(13) Ono, H.; Ishimaru, S.; Ikeda, R.; Ishida, H. *Bull. Chem. Soc. Jpn.* **1997**, *70*, 2963−2972.
(14) Mallikarjunaiah, K. J.; Damle, R.; Ramesh, K. P. *Solid State Nucl. Magn. Reson.* **2008**, *34*, 180−185.
(15) Matthews, C. H.; Gilson, D. F. R. *Can. J. Chem.* **1970**, *48*, 2625−2627.
(16) McBrierty, V. J.; Douglass, D. C.; Wudl, F. *Solid State Commun.* **1982**, *43*, 679−682.
(17) Hoeptner, W.; Mehring, M.; Von, J. U., S.; Wolf, H. C.; Morra, B. S.; Enkelmann, V.; Wegner, G. *Chem. Phys.* **1982**, *73*, 253−261.
(18) Rojo, T.; Arriortua, M. I.; Ruiz, J.; Darriet, J.; Villeneuve, G.; Beltran-Porter, D. *J. Chem. Soc., Dalton Trans.* **1987**, 285−291.
(19) Pajak, Z.; Kozak, A.; Grottel, M. *Solid State Commun.* **1988**, *65*, 671−673.
(20) Rojo, T.; Mesa, J. L.; Arriortua, M. I.; Savariault, J. M.; Galy, J.; Villeneuve, G.; Beltran, D. *Inorg. Chem.* **1988**, *27*, 3904−3911.
(21) Burbach, G.; Dou, S.-Q.; Weiss, A. *Ber. Bunsen-Ges. Phys. Chem.* **1989**, *93*, 1302−1309.
(22) Grottel, M.; Kozak, A.; Koziol, A. E.; Pajak, Z. *J. Phys.: Condens. Matter* **1989**, *1*, 7069−7083.
(23) Burbach, G.; Weiden, N.; Weiss, A. *Z. Naturforsch., A: Phys. Sci.* **1992**, *47a*, 689−701.
(24) Kozak, A.; Grottel, M.; Wasicki, J.; Pajak, Z. *Phys. Status Solidi A* **1994**, *141*, 345−352.
(25) Ono, H.; Ishimaru, S.; Ikeda, R.; Ishida, H. *Ber. Bunsen-Ges. Phys. Chem.* **1998**, *102*, 650−655.
(26) Ono, H.; Ishimaru, S.; Ikeda, R.; Ishida, H. *Bull. Chem. Soc. Jpn.* **1999**, *72*, 2049−2054.
(27) Wasserscheid, P.; Welton, T. *Ionic Liquids in Synthesis*; VCH-Wiley: Weinheim, Germany, 2003.
(28) Ohno, H. *Electrochemical Aspects of Ionic Liquids*; Wiley-Interscience: Hoboken, NJ, 2005.
(29) Endo, T.; Widgeon, S.; Yu, P.; Sen, S.; Nishikawa, K. *Phys. Rev. B* **2012**, *85*, 054307/1−054307/9.
(30) Endo, T.; Kato, T.; Tozaki, K.; Nishikawa, K. *J. Phys. Chem. B* **2010**, *114*, 407−411.
(31) Endo, T.; Murata, H.; Imanari, M.; Mizushima, N.; Seki, H.; Nishikawa, K. *J. Phys. Chem. B* **2012**, *116*, 3780−3788.
(32) Endo, T.; Kato, T.; Nishikawa, K. *J. Phys. Chem. B* **2010**, *114*, 9201−9208.
(33) Van Geet, A. L. *Anal. Chem.* **1968**, *40*, 2227−2229.
(34) Van Geet, A. L. *Anal. Chem.* **1970**, *42*, 679−680.
(35) Raiford, D. S.; Fisk, C. L.; Becker, E. D. *Anal. Chem.* **1979**, *51*, 2050−2051.
(36) Ammann, C.; Meier, P.; Merbach, A. *J. Magn. Reson.* **1982**, *46*, 319−321.
(37) Abragam, A. *Principles of Nuclear Magnetism*; Oxford University Press: Oxford, U.K., 1961.
(38) Frisch, M. J.; Trucks, G. W.; Schlegel, H. B.; Scuseria, G. E.; Robb, M. A.; Cheeseman, J. R.; Scalmani, G.; Barone, V.; Mennucci, B.; Petersson, G. A.; Nakatsuji, H.; Caricato, M.; Li, X.; Hratchian, H. P.; Izmaylov, A. F.; Bloino, J.; Zheng, G.; Sonnenberg, J. L.; Hada, M.; Ehara, M.; Toyota, K.; Fukuda, R.; Hasegawa, J.; Ishida, M.; Nakajima, T.; Honda, Y.; Kitao, O.; Nakai, H.; Vreven, T.; Montgomery, J. A., Jr.; Peralta, J. E.; Ogliaro, F.; Bearpark, M.; Heyd, J. J.; Brothers, E.; Kudin, K. N.; Staroverov, V. N.; Keith, T.; Kobayashi, R.; Normand, J.; Raghavachari, K.; Rendell, A.; Burant, J. C.; Iyengar, S. S.; Tomasi, J.; Cossi, M.; Rega, N.; Millam, J. M.; Klene, M.; Knox, J. E.; Cross, J. B.; Bakken, V.; Adamo, C.; Jaramillo, J.; Gomperts, R.; Stratmann, R. E.; Yazyev, O.; Austin, A. J.; Cammi, R.; Pomelli, C.; Ochterski, J. W.; Martin, R. L.; Morokuma, K.; Zakrzewski, V. G.; Voth, G. A.; Salvador, P.; Dannenberg, J. J.; Dapprich, S.; Daniels, A. D.; Farkas, O.; Foresman, J. B.; Ortiz, J. V.; Cioslowski, J.; Fox, D. J. *Gaussian 09*; Gaussian, Inc.: Wallingford, CT, 2010.
(39) Becke, A. D. *J. Chem. Phys.* **1993**, *98*, 5648−5652.
(40) Lee, C.; Yang, W.; Parr, R. G. *Phys. Rev. B* **1988**, *37*, 785−789.
(41) Miehlich, B.; Savin, A.; Stoll, H.; Preuss, H. *Chem. Phys. Lett.* **1989**, *157*, 200−206.
(42) Hayashi, S.; Ozawa, R.; Hamaguchi, H. *Chem. Lett.* **2003**, *32*, 498−499.
(43) Umebayashi, Y.; Fujimori, T.; Sukizaki, T.; Asada, M.; Fujii, K.; Kanzaki, R.; Ishiguro, S. *J. Phys. Chem. A* **2005**, *109*, 8976−8982.
(44) Hunt, P. A. *J. Phys. Chem. B* **2007**, *111*, 4844−4853.
(45) Tsuzuki, S.; Arai, A. A.; Nishikawa, K. *J. Phys. Chem. B* **2008**, *112*, 7739−7747.
(46) Parsons, D. F.; Ninham, B. W. *J. Phys. Chem. A* **2009**, *113*, 1141−1150.
(47) Endo, T.; Tozaki, K.; Masaki, T.; Nishikawa, K. *Jpn. J. Appl. Phys.* **2008**, *47*, 1775−1779.
(48) Van Vleck, J. H. *Phys. Rev.* **1948**, *74*, 1168−1183.
(49) Choudhury, A. R.; Winterton, N.; Steiner, A.; Cooper, A. I.; Johnson, K. A. *J. Am. Chem. Soc.* **2005**, *127*, 16792−16793.
(50) Holbrey, J. D.; Reichert, W. M.; Nieuwenhuyzen, M.; Johnston, S.; Seddon, K. R.; Rogers, R. D. *Chem. Commun.* **2003**, 1636−1637.
(51) Andre, M.; Loidl, J.; Laus, G.; Schottenberger, H.; Bentivoglio, G.; Wurst, K.; Ongania, K. H. *Anal. Chem.* **2005**, *77*, 702−705.
(52) Ibers, J. A.; Stevenson, D. P. *J. Chem. Phys.* **1958**, *28*, 929−938.
(53) Gutowsky, H. S.; Pake, G. E. *J. Chem. Phys.* **1950**, *18*, 162−170.
(54) Bloembergen, N.; Purcell, E. M.; Pound, R. V *Phys. Rev.* **1948**, *73*, 679−712.
(55) Morrow, T. I.; Maginn, E. J. *J. Phys. Chem. B* **2002**, *106*, 12807−12813.
(56) Zhao, W.; Leroy, F.; Heggen, B.; Zahn, S.; Kirchner, B.; Balasubramanian, S.; Mueller-Plathe, F. *J. Am. Chem. Soc.* **2009**, *131*, 15825−15833.
(57) Dupont, J.; Suarez, P. A. Z. *Phys. Chem. Chem. Phys.* **2006**, *8*, 2441−2452.
(58) Yang, J.-Z.; Lu, X.-M.; Gui, J.-S.; Xu, W.-G. *Green Chem.* **2004**, *6*, 541−543.
(59) Triolo, A.; Russina, O.; Hardacre, C.; Nieuwenhuyzen, M.; Gonzalez, M. A.; Grimm, H. *J. Phys. Chem. B* **2005**, *109*, 22061−22066.
(60) Antony, J. H.; Mertens, D.; Dölle, A.; Wasserscheid, P.; Carper, W. R. *ChemPhysChem* **2003**, *4*, 588−594.
(61) Carper, W. R.; Wahlbeck, P. G.; Dölle, A. *J. Phys. Chem. A* **2004**, *108*, 6096−6099.
(62) Antony, J. H.; Mertens, D.; Breitenstein, T.; Dölle, A.; Wasserscheid, P.; Carper, W. R. *Pure Appl. Chem.* **2004**, *76*, 255−261.
(63) Carper, W. R.; Wahlbeck, P. G.; P., G.; Antony, J. H.; Mertens, D.; Dölle, A.; Wasserscheid, P. *Anal. Bioanal. Chem.* **2004**, *378*, 1548−1554.
(64) Rivera, A.; Brodin, A.; Pugachev, A.; Rössler, E. A. *J. Chem. Phys.* **2007**, *126*, 114503.
(65) Shamim, N.; McKenna, G. B. *J. Phys. Chem. B* **2010**, *114*, 15742−15752.
(66) Fan, W.; Zhou, Q.; Sun, J.; Zhang, S. *J. Chem. Eng. Data* **2009**, *54*, 2307−2311.
(67) Tokuda, H.; Hayamizu, K.; Ishii, K.; Susan, M. A. B. H.; Watanabe, M. *J. Phys. Chem. B* **2004**, *108*, 16593−16600.
(68) Machida, H.; Taguchi, R.; Sato, Y.; Smith, R. L., Jr. *Fluid Phase Equilib.* **2009**, *281*, 127−132.
(69) Wadell, H. *J. Geol.* **1935**, *43*, 250−280.
(70) Blinc, R.; Lahajnar, G. *J. Chem. Phys.* **1967**, *47*, 4146−4152.
(71) Makrocka-Rydzyk, M.; Glowinkowski, S.; Jurga, S.; Meyer, W. H. *Appl. Magn. Reson.* **2000**, *18*, 63−70.
(72) Johnson, R. D.; Yannoni, C. S.; Dorn, H. C.; Salem, J. R.; Bethune, D. S. *Science* **1992**, *255*, 1235−1238.